

A skew quadrupole for the AGS to minimize the polarization losses of the polarized beams

N. Tsoupas

March 2022

Collider Accelerator Department
Brookhaven National Laboratory

U.S. Department of Energy

USDOE Office of Science (SC), Nuclear Physics (NP) (SC-26)

Notice: This technical note has been authored by employees of Brookhaven Science Associates, LLC under Contract No. DE-SC0012704 with the U.S. Department of Energy. The publisher by accepting the technical note for publication acknowledges that the United States Government retains a non-exclusive, paid-up, irrevocable, world-wide license to publish or reproduce the published form of this technical note, or allow others to do so, for United States Government purposes.

DISCLAIMER

This report was prepared as an account of work sponsored by an agency of the United States Government. Neither the United States Government nor any agency thereof, nor any of their employees, nor any of their contractors, subcontractors, or their employees, makes any warranty, express or implied, or assumes any legal liability or responsibility for the accuracy, completeness, or any third party's use or the results of such use of any information, apparatus, product, or process disclosed, or represents that its use would not infringe privately owned rights. Reference herein to any specific commercial product, process, or service by trade name, trademark, manufacturer, or otherwise, does not necessarily constitute or imply its endorsement, recommendation, or favoring by the United States Government or any agency thereof or its contractors or subcontractors. The views and opinions of authors expressed herein do not necessarily state or reflect those of the United States Government or any agency thereof.

1 A Skew Quadrupole for the AGS to minimize the
2 Polarization losses of the Polarized Beams*

3 N. Tsoupas[†], V. Badea, S. Belavia, H. Huang, D. Lehn, R. Lynch,
4 G. Mahler, I. Marneris, J. Sandberg, V. Schoefer, J. Tuozzolo

5 *Brookhaven National Laboratory, Collider-Accelerator Department, Upton, LI, NY*
6 *11973, USA*

7 **Abstract**

8 The partial helices installed in the Alternating Gradient Synchrotron (AGS)
9 [1] eliminate both, the imperfection and the vertical intrinsic spin resonances
10 thus yielding a 70% polarized proton beam with rigidity 79.4 [Tm] with
11 2×10^{11} protons/bunch at the end of the AGS acceleration cycle.

12 The initial beam polarization at the exit of the 200 MeV Linac is measured to
13 be 80%. The 10% loss of the polarization at the end of the AGS acceleration
14 cycle is due to the horizontal spin resonances which are caused by the beta-
15 tron oscillations of the beam in the presence of the partial helices. To reduce
16 the effect of these horizontal spin resonances on the beam polarization, the
17 “jump Quads method” is applied in the AGS [2] which eliminates, almost
18 all, the horizontal spin resonances and increases the final polarization of the
19 proton beam to the value of 70%. A study [3] shows that these horizontal
20 spin resonances can be totally eliminated by introducing into the AGS ring,
21 skew quadrupoles which linearly couple the beam motions to excite new hori-
22 zontal spin resonances which minimize the horizontal-spin-resonances caused
23 by the partial-helices.

24 These skew quadrupoles are excited during the time the polarized beam
25 crosses these horizontal spin resonances. The time interval of the spin-
26 resonance-crossing is of the order of a millisecond and this requires that the
27 material of the skew quadrupoles is made of ferrite or of laminated iron to
28 minimize the eddy currents in the conductive parts of the skew quadrupoles.

29 In this technical note we provide results from the electromagnetic design
30 [4] of the Skew Quadrupole. This study includes the calculation of the mag-
31 netic multipoles of the quadrupole and the Ohmic losses in the coils and all
32 the conductive parts of the quadrupoles including the 0.025” thick lamina-

*Work supported by the US Department of Energy

[†]tsoupas@bnl.gov

33 tions of the quadrupole. This study presents also results of the presence of
34 the beam pipe on the magnetic field at the region of the circulating beam.
35 The information provided in this technical note should be sufficient for the
36 reader to reproduce a 3D model of the skew quadrupole and introduce it in
37 the OPERA computer code [4] to obtain the results presented in this paper.
38 This quadrupole will be used in the AGS ring as a skew quadrupole and will
39 be referred in this paper as either skew quadrupole or simply quadrupole.

40

41 *Keywords:* Iron laminated quadrupole magnet

42 1. Introduction

43 As part of the EIC project [5] a Research and Development (R&D) effort
44 is under way to increase the polarization of the polarized beams accelerated
45 in the EIC complex with the goal to maximize the polarization value of the
46 polarized proton beam to a value larger than 70% at the final EIC proton
47 energy of 275 GeV.

48 At the present time the AGS synchrotron is equipped with two partial he-
49 lices [1] which totally eliminate both the imperfection and the vertical intrinsic
50 spin resonances which occur during the acceleration of polarized protons
51 to a final beam rigidity of 79.4 [Tm] with 2×10^{11} protons/bunch yielding a
52 65% final polarization of the proton beam.

53 Although the two partial helices eliminate the imperfection and the vertical
54 intrinsic vertical spin resonances, they fall short in eliminating the horizontal
55 spin resonances. These horizontal spin resonances occur through the interaction
56 of the beam's betatron oscillations with the magnetic field of the partial
57 helices.

58 To overcome the horizontal spin resonances the method of "jump Quads" [2]
59 is currently being used and the polarization of the beam increases to 70%.
60 To further increase the polarization of the extracted beam from the AGS,
61 by totally eliminating the horizontal spin resonances, two methods were pro-
62 posed; The method of using four partial helices in AGS [6] and the method
63 of using skew quadrupoles in the AGS ring [3].

64 Although theoretical studies show that either method totally eliminates the
65 horizontal spin resonances the skew quadrupoles method [3] was chosen.

66 The skew quadrupole method is based on the linear coupling introduced by
67 the skew quadrupoles which can excite horizontal spin resonances that can-

68 cel the ones caused by the partial helices.
 69 The skew quadrupoles are being used and placed at specific locations on the
 70 available space along the straight sections of the AGS. A perspective view of
 71 the skew quadrupole is shown in Fig. 1.
 72 In this technical note a brief description of the mechanical design of the skew
 73 quadrupole is given, and some of the results from the electromagnetic study
 74 of the quadrupole are presented. Namely the magnetic multipoles at a radius
 75 $R=2$ cm, the Ohmic losses including those losses caused by the eddy currents
 76 in the coil-conductors and the conducting parts of the quadrupole like the
 77 iron laminations.
 78 The electromagnetic study utilizes the 3D-AC-steady state electromagnetic
 79 module of the OPERA computer code [4]. In addition the 3D transient
 80 electromagnetic module of the OPERA computer code is used to reproduce
 81 with better accuracy the magnetic field and the Ohmic losses during the
 82 actual operation of the skew quadrupoles. Results from both studies, the
 83 AC-steady-state and the transient study are presented.

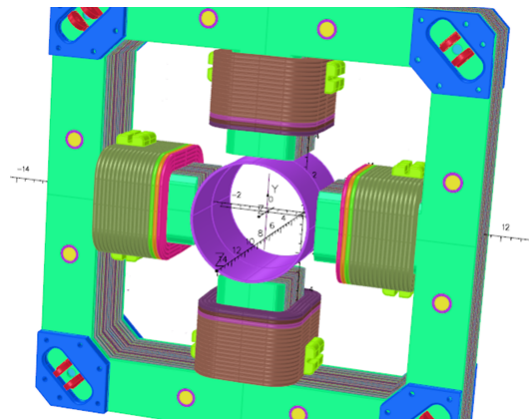


Figure 1: A perspective view of the skew quadrupole. A 3D drawing in “igs” format is imported to the OPERA code which performs the electromagnetic calculations. The green objects are 1/4” thick plates made of magnetic iron to retain the 0.025” thick laminations within the plates. The little green objects on the outer surfaces of the coils are conducting masses made of aluminum to abduct the heat generated by the coils. This heat abductured by the aluminum masses is removed by water running inside copper tubing which is thermally epoxy-bonded to the aluminum cooling blocks. The copper tubing is not shown in this drawing.

84 2. Mechanical Considerations of the Skew-Quadrupole

85 As mentioned earlier the skew quadrupoles will be positioned in available
86 spaces within the straight sections of the AGS ring.

87 Such spaces are rather short because all the straight sections are occupied by
88 other devices like tune-quadrupoles chromaticity-sextupoles, or other devices
89 which leave only a limited space for the skew quadrupoles.

90 Fig. 2 is a picture of the available space of 17.5 cm in length for the place-
91 ment of the skew quadrupole. On the left side of the picture in Fig. 2 are the
92 coils (grey objects), and the iron yoke (green object) of the AGS main mag-
93 net and on the right side of the picture is one of the chromaticity sextupoles
94 of the AGS. The space between the AGS main magnet and the sextupole is
95 for the placement of the skew quadrupole.

96 The drawing in Fig. 3 on the left is a projection of the skew quadrupole on a
97 plane normal the beam direction, and the drawing on the right is a projection
98 of the quadrupoles on a horizontal plane. A 3D drawing of the quadrupole
99 is shown in Fig. 1. The following is a list of items of some of the geometrical
100 constrains that have been applied in the design of the skew quadrupole.

101

- 102 • the length of the quadrupole including the coils, along the beam direc-
103 tion, should occupy a length no greater than 16.51 cm
- 104 • the iron core of the quadrupole magnet is of laminated steel of 0.025”
105 thick to reduce the eddy currents.
- 106 • the 0.25” thick end-plates showing in green in Fig. 1 are to hold the
107 laminations together.
- 108 • the coils should be as far as possible from the center of the quadrupole
109 to reduce the ohmic losses on the coils due to the eddy currents.
- 110 • the aperture of the quadrupole should be adequate for the quadrupole
111 to be placed over the beam pipe of the AGS.
- 112 • Each of the 17 turns of the conductor is separated in four isolated
113 conductors inside the coil to reduce the eddy currents and minimize

114
115

the Ohmic losses due to eddy currents. Each set of the four conductors are electrically connected at the entrance and exit of the coil¹.

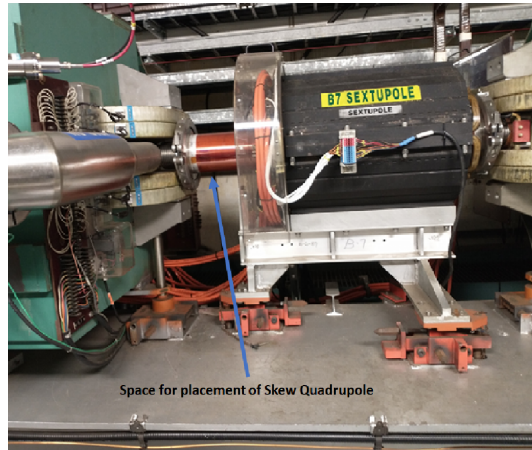


Figure 2: A picture of the B7 straight section of the AGS. The Skew Quadrupole will be placed in the available straight section between the AGS main magnet (green object on the left) and the chromaticity sextupole on the right.

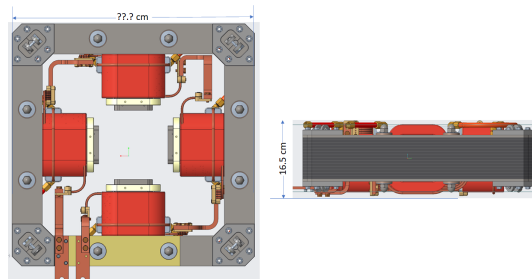


Figure 3: Two 2D drawings of the skew quadrupole. The drawing on the left is a projection on a plane normal to the beam direction, and the one on the right is a projection on a plane which includes the beam direction.

116
117

Table 1 shows some dimensions of the skew quadrupole including some information on the coils.

¹A technical note on this quadrupole will report more details on the mechanical design of this skew quadrupole.

Table 1: Table Some dimensions of the skew quadrupole

Ap-Radius [cm]	Length [cm]	Width [cm]	Vacuum pipe wall [mm]	Coil-turns	Cond/turn
8.5	16.5	35	3	17	4

118 **3. Electrical connections and shape of the current pulse to excite**
 119 **the Skew-Quadrupole**

120 Each of the skew quadrupoles will be excited during the time the beam
 121 crosses an horizontal spin resonances. Such time corresponds to the beam
 122 momentum which satisfies the condition $G\gamma = Q_x + n$ where Q_x is the hori-
 123 zontal tune and n is an integer.

124 Each quadrupole will be powered by its own power supply and will generate
 125 a pulse of a given amplitude for each crossing over a spin resonance during
 126 the AGS acceleration cycle.

127 The red trace shown in Fig. 4 is a schematic shape of a current pulse which
 128 will be generated as the beam crosses each horizontal spin resonance. The
 129 amplitude of the current pulse will vary depending on the strength of the
 130 horizontal spin resonance the beam crosses.

131 Fig 5 is a typical plot of the current pulses of an individual skew-quadrupole
 132 during the acceleration cycle. Note that the current pulses have varied am-
 133 plitude and are either positive or negative in value.

134 The four coils of each skew quadrupole are connected in series and the two
 135 conductor leads at the bottom of the picture are connected to a bipolar power
 136 supply. The drawing on the left in Fig 6 shows the wire connection of the
 137 four coils. The “cooling pipes” on this drawing are made of copper material
 138 and abduct the heat from the cooling aluminum blocks which are in contact
 139 with each of the coils. The aluminum masses which abduct the heat from the
 140 coils are electrically insulated from the conductors of the coils. The draw-
 141 ing on the right is a cross section of the coil which shows that each turn of
 142 the coil consists of four electrical isolated conductors which are electrically
 143 connected at the entrance and exit of each coil. This splitting of each turn
 144 into four conductors and their electrical isolation of these four conductors
 145 inside the coil reduces the eddy currents which results in the reduction of the
 146 Ohmic losses generated by the coil. The copper masses which abduct the heat
 147 from the Ohmic losses of the coils are also shown on the left drawing of Fig 6.

148

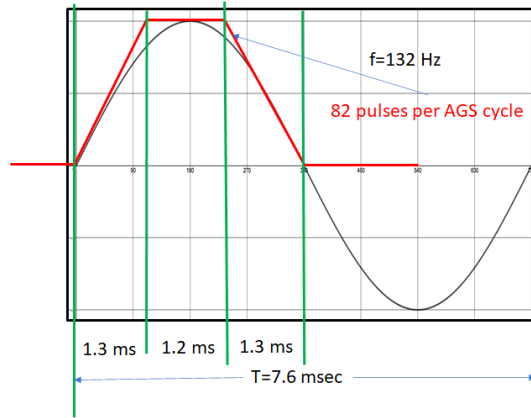


Figure 4: The red trace represent a typical current pulse which excites the quadrupoles at the time interval the beam crosses an horizontal spin resonance. The amplitude of these pulses varies depending the strength of the horizontal spin resonance to cancel.

149

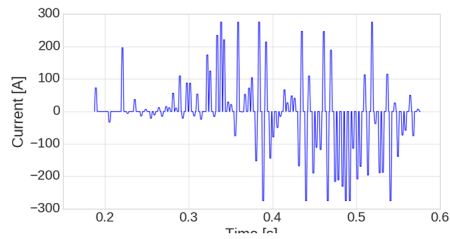


Figure 5: A typical set of current pulses which excite an individual skew quadrupole during an AGS cycle. The amplitude of each current pulse which excites the skew quadrupole is different for each horizontal spin resonance.

150

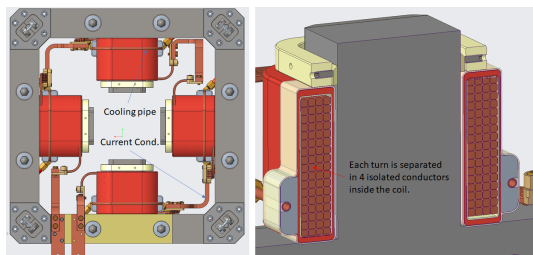


Figure 6: The left picture shows the conductors which are used for the electrical connection of the coils. The pipes which carry the cooling water of the “cooling copper” blocks are also shown. The left picture shows the quadrupole cut in half with a plane normal to the longitudinal axis of the quadrupole. This picture shows the 17 turns of the coil. Each turn consists of four electrically isolated conductors 0.23 cmx0.23 cm in cross section each. The four conductors of each turn are electrically connected only at the entrance and exit of each of the four coils of the quadrupole but they are electrically isolated inside each coil.

151 **4. Modeling the Skew-Quadrupole for the Electromagnetic Calculations**
 152

153 Only 3D electromagnetic calculations were performed on the skew quadrupole
 154 by the use of the OPERA computer code. Due to the relatively low B-
 155 field in the magnetic material all the calculations were performed with a
 156 constant permeability $\mu=4000$ for all the magnetic material involved in the
 157 calculations. The reason of using constant permeability is due to the very
 158 large number of nodes used in the OPERA code calculations to describe the
 159 quadrupole model that otherwise would require weeks of calculations instead
 160 of three to four days required when the quadrupole is modeled with constant
 161 permeability. The 2D calculations were excluded for two reasons, first,
 162 the length of the magnet was short compared to the aperture-radius of the
 163 quadrupole, therefore no constant gradient values were generated within the
 164 quadrupole, and second the normalized beam emittance of 15π [mm.mrad]
 165 makes a beam size, even at injection beam energies into the AGS, much
 166 smaller as compared to the aperture (R=8.05 cm) of the quadrupole there-
 167 fore all the multipoles, higher than the quadrupole multipole, at the beam
 168 radius are not significant and there was no reason to shape the pole faces
 169 of the quadrupole to minimize the 12-pole multipole which is the first al-
 170 lowed multipole. The maximum integrated quadrupole field required to be
 171 generated by the quadrupole is 0.2 [T]. Given that the iron length of the
 172 quadrupoles is 11.45 cm and the radius of the quadrupole’s aperture is 8.05
 173 cm the maximum a pole tip magnetic field of the quadrupole should be ~ 0.14

174 [T]. Although such a pole tip magnetic field is low enough for the quadrupole
 175 to be constructed by ferrite material which saturates at 0.3 [T] the decision
 176 was made for the quadrupole to be fabricated with 0.025” thick iron lamina-
 177 tions. The iron laminations allow for stronger gradient in the quadrupole due
 178 to higher saturation of ~ 1.7 T in the iron, the eddy currents generated in the
 179 laminations result in Ohmic losses which are part of the study in this paper.
 180 The results from this study provides information on the effect of the eddy
 181 currents, generated in all conductive parts of the quadrupole, on the main
 182 quadrupole field and also on the ohmic losses on the conductive materials of
 183 the quadrupole. The skin depth δ of the electromagnetic field in magnetic
 184 iron at the frequency of 135 Hz is given by the formulae

$$\delta = 503 \left(\frac{1}{f \sigma \mu_r} \right)^{1/2} \quad (1)$$

185 In the equation above the skin depth δ is in [m] the frequency f in Hz the
 186 conductivity σ is in $(\Omega\text{m})^{-1}$ and μ_r is the relative permeability of the iron.
 187 Fig 7 is a plot of the skin depth vs frequency for various materials.
 188 From this plot one can estimate that the skin depth in magnetic iron like
 189 “Si-Fe” for the frequency of 135 Hz is 0.17 mm. The lamination thickness
 190 used in the quadrupole is 0.63 mm which is not much larger as compared to
 191 the the skin depth of 0.17 mm. In the OPERA model of the quadrupole each
 192 0.063 cm thick lamination is electrically isolated from the neighboring one, in
 193 additions to make the calculations more accurate each 0.63 mm thick lami-
 194 nation is split into two $0.63/2$ mm= 0.315 mm thick entities and the distance
 195 between two neighboring nodes in the OPERA model was set to “quadratic”
 196 thus further increasing the accuracy of the calculations.
 197 In such a thin lamination if the magnetic field is parallel to the large surface
 198 of the lamination the eddy currents which will be created in the lamina-
 199 tion, will partially cancel each other inside the lamination. However for a
 200 short quadrupole the direction of the magnetic field is not parallel to the
 201 laminations but there is a component of the B-field which is normal to the
 202 laminations. This component of the field generates additional eddy currents
 203 inside the laminations which do not cancel each other. To explain graphically
 204 the above sentences related to eddy currents cancelation or non cancelation
 205 we refer to Fig 8. The figure on the left shows the magnetic field direction
 206 parallel to the lamination. The change of the magnetic field generates eddy
 207 currents in and out of the page. If the width of the lamination is compa-
 208 rable to the skin depth there will be some cancelation of the eddy currents.

209 However if the direction of the magnetic field is not parallel to the lamina-
 210 tion like in the left figure of Fig. 8 the change of the B_x component of the
 211 field will generate eddy currents which will not cancel each other because the
 dimension “L” of the lamination is long compared to the skin depth.

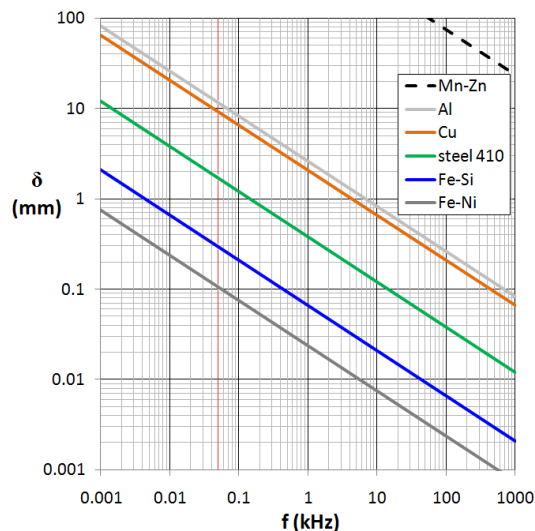


Figure 7: A plot of the skin depth of the electromagnetic wave versus frequency in various materials embedded in such EM waves. The skin depth in the material used for this quadrupole at $f=135$ Hz is ~ 0.17 mm.

212

213 5. Purpose of the Electromagnetic calculations on the Skew-Quadrupole

214 Given that the quadrupole will operate in a transient mode as shown
 215 by the red trace in Fig. 4, the purpose of the electromagnetic field study is
 216 to obtain results to determine the following physical quantities during the
 217 operation of the quadrupole.

- 218 • The integrated quadrupole field as a function of time
- 219 • The Ohmic losses in the coils
- 220 • The Ohmic losses in the 0.025” thick laminations
- 221 • The Ohmic losses in the 0.25” thick end plates
- 222 • The integrated field multipoles at the radius of the beam

223
224

- The effect of the eddy currents generated in the material of the vacuum pipe on the magnetic field at the region of the circulating beam

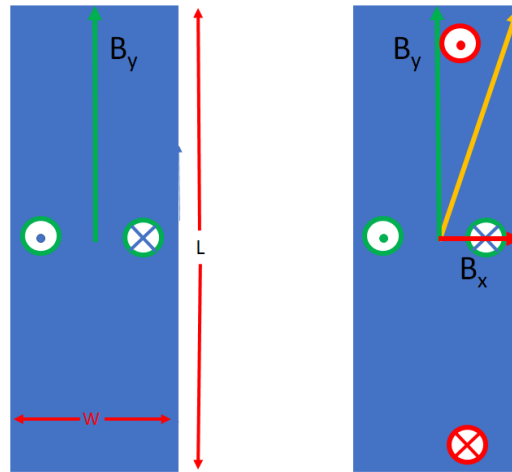


Figure 8: The B_y field on the left figure is parallel to the surface of the lamination. The change of the B_y field will generate eddy currents which will partially cancel each other if the width of the lamination is comparable to the skin depth. In the right picture the B-field is not parallel to the surface of the lamination and the change in time of the B_x component of the B-field which is normal to the surface of the lamination will generate eddy currents (red circles) which will not cancel each other if the dimension “L” of the lamination is much larger than the skin depth.

225
226
227
228
229
230
231
232
233
234
235
236
237
238

The opera computer code has the capability to determine all the quantities in the list above. There are two modules in the OPERA computer code which can be used; namely the AC steady state module and the transient module. The frequency of the sinusoidal AC steady state current which is close to a single transient pulse (red trace) shown in figure Fig. 4 is $f=135$ Hz. The results from the AC steady state solution are very conservative and correspond to almost 40 times of the Ohmic losses as compared to the actual operation of the skew quadrupoles which is a set of pulses, over an AGS cycle, of varying amplitude shown in Fig. 5. Before we proceed with the results from the OPERA solutions a brief explanation, on modeling the iron laminations in the OPERA code is provided below.

The drawing on the right of Fig. 9 is a projection of the skew quadrupole on a plane normal to the laminations of the quadrupole. The left side of Fig. 9 is a schematic diagram of only three of the 160 iron laminations. Each

239 iron lamination is 0.025" thick and is electrically isolated by an infinitely
 240 thin layer (OPERA's feature) from the adjacent lamination. In addition,
 241 as part of the OPERA model-design, each laminations is split in the middle
 242 thus each laminations is made of two laminations of 0.0125" thick electrically
 243 connected. The distance between two adjacent nodes has been set to 0.05"
 244 "quadratic" which in effect reduces the node-distance and increases the ac-
 245 curacy of the calculations. Although the "layering" feature of the OPERA
 246 model could have been used to split each lamination into thinner ones, it was
 247 decided to simply split each 0.025" thick lamination in two. The "Geometric
 248 layering" feature of the OPERA is being used for the 0.25" thick "holding
 249 plates" (green material in Fig. 1) where two thin layers of 0.025 cm thick
 250 at either of the large surfaces of the plates are being used. Table 2 displays
 251 some properties of the materials the quadrupole is made of which are relevant
 252 in the OPERA model calculations. Other nonconductive and nonmagnetic
 253 material which are used in the structure of the magnet are not significantly
 254 contributing to magnetic field distribution of the magnet at these frequencies
 255 of 135 Hz.

256 *5.1. Results from the AC Steady State Calculations at f=135 Hz*

257 The AC steady state calculations were performed by using the frequency
 258 of 135 Hz because it is the best frequency which fits the transient pulse as
 259 shown in Fig. 4. It is the sinusoidal black trace which better fits one of the
 260 single transient pulses which excites the skew quadrupole at the time the
 261 beam crosses the horizontal spin resonances.

262 The OPERA model was made in IGS format which was imported into the
 263 OPERA code. Fig. 10 is a perspective view of the 1/8th size 3D model used
 264 in the OPERA computer code.

265 The plot of the B_x field at a phase angle of 90° and $R=1$ cm from the axis of
 266 the quadrupole is shown in Fig. 11. From this plot the integrated quadrupole
 267 field $\int_{-\infty}^{+\infty} B_Q dz$ of the skew quadrupole is calculated to be 0.215 T when
 268 the quadrupole is excited at a current of 185 A. This integrated field is
 269 slightly larger than the required maximum field of 0.19 [T]. From this plot
 270 of the B_x field vs z distance, it appears that there is no "uniform quadrupole
 271 field" along the length of the quadrupole because the small L/R ratio of the
 272 quadrupole.

273 From the Fourier analysis of the radial B_r field calculated at a radius of 4
 274 cm it is concluded that the 12th pole component of the field which is the first
 275 allowed multipole of the quadrupole is less than 0.003% of the quadrupole

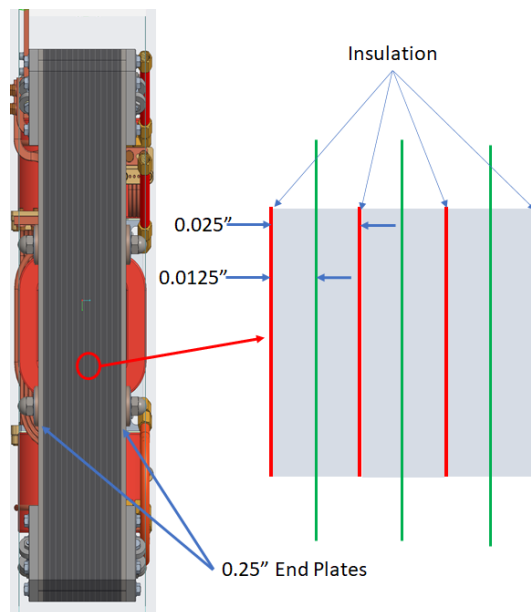


Figure 9: A schematic diagram showing the boundaries (red lines) of the 0.025" thick laminations. The insulation (red line) is of zero thickness. Each 0.025" thick lamination is electrically isolated from the next and is made of two entities electrically connected, 0.0125" thick each, in the model. The green line shows schematically the separation of each lamination in two 0.0125" thick laminations.

276 field. This justifies the reason that the pole faces of the quadrupole were not
 277 mechanically shaped to minimize the 12-pole component of the field.
 278 In addition to the quadrupole field and its quality generated by the quadrupole,
 279 another important physical quantity from the operation of the skew quadrupole
 280 is the power dissipation in the conductive parts of the quadrupole like, lam-
 281 inations, end-holding plates, and the main coils. These quantities appear
 282 in Table 3.

283 Although these quantities of average power dissipation during the AC steady
 284 state operation may appear excessive, especially for a non-water-cooled con-
 285 ductor coil, in the actual operation of the quadrupole these quantities are very
 286 small because the duty cycle of the actual operation of the skew quadrupole
 287 in AGS is $1/40^{th}$ of the duty cycle of the steady state operation at 135 Hz.

288 To speed up the calculations and check for any errors the initial OPERA
 289 model of the quadrupole used a coarse mesh. As the grid size of the mesh
 290 in the various parts of the model was decreasing so the average power dis-
 291 sipation in the coils, the holding plates, and the laminations. At a grid size

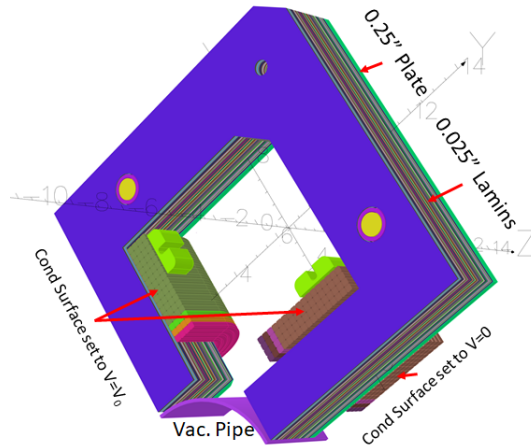


Figure 10: A perspective view of 1/8th model of the quadrupole's 3D model used in the OPERA computer calculations. The z=0 symmetry plane cuts the 17x4 conductors of each coil and exposes 17x4 conductor-surfaces of each coil as shown in the figure. These conductor surfaces were assigned the voltage $V=V_0$ Volts. The other conductor surfaces which were exposed from the cut by the symmetry planes $y=0$ and $x=0$ were set to $V=0$ Volts.

292 of 0.4" and below in the coil, the power dissipation in the coil remained con-
 293 stand, the same was also for the power dissipation in the holding plates for
 294 grid sizes 0.06" and 0.05". But this was not the case for the grid size in
 295 the laminations where the power dissipation was still projected to decrease
 296 for grid size below the value of 0.05". However it was not possible to de-
 297 crease the grid size in the laminations at a lower value than 0.05" because
 298 the model could not be meshed in either the 128 RAM PC or the 128 RAM
 299 UNIX computer.

300 In an attempt to provide a more accurate value for the power dissipation in
 301 the laminations the OPERA quadrupole model run for various grid sizes in
 302 the laminations ranging from 0.4" to 0.05" and a plot of power dissipation
 303 vs grid size in the laminations was made and the data points were fitted by a
 304 polynomial to obtain the power dissipation for very small grid size. Unfortu-
 305 nately this method did not work because it was yielding a "negative power
 306 dissipation" at the limit of grid size approaching to zero.

307 A communication with the OPERA consultants will soon start to explore
 308 the reason why the model cannot be meshed with the grid size smaller than
 309 0.05".

310 The average power in each of the 80 lamination lamination when the

Table 2: Material properties used in the OPERA model of the quadrupole

Material	conductivity [Ωm] ⁻¹	Thickness [cm]	μ
Laminations	1×10^7	0.0635	4000
Iron Plates	1.0×10^7	0.635	4000
Coil-Conductor	5.89×10^7	0.519×0.519	1.0
Vac-Pipe	1.0×10^7	0.3	1.0

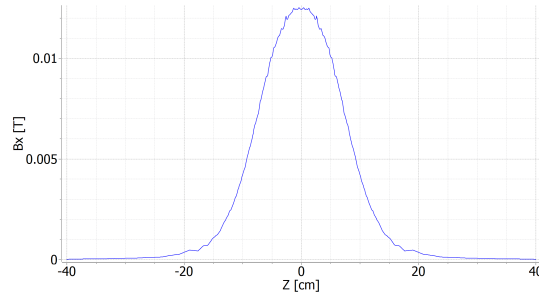


Figure 11: The B_x field at $R=1$ cm of the skew Quadrupole at 90° phase. The integrated quadrupole at this phase of 90° is 0.22 [T]. From this plot it appears that the ratio L/R of this quadrupole is too small to provide a uniform quadrupole field along the length of the quadrupole.

311 quadrupole is running in an AC steady state with frequency of 135 Hz
 312 plotted in Fig. 12 which plots the average power dissipation in each 0.025”
 313 thick lamination. The power dissipation on the other 80 laminations down-
 314 stream, is a mirror image of the Fig. 12. It is worth noticing that the power
 315 dessipation in each lamination increases with the distance from the center of
 316 the magnet. This increase in the power is due to the eddy currents which are
 317 created by the time varying B-field component which is normal to the surface
 318 of the lamination as shown in Fig. 8. The power dissipation in the Coils the
 319 lamination and the holding-plates also appears in Table 3. Given that the

Table 3: Results from the 3D AC steady state calculations

I_{max}	$L_{(Induct.)}$	$\int B_Q dz$	Average Power		
			Coil	Lam	Plate
[A]	[mH]	[T]	[W]	[W]	[W]
185	0.64	0.21	725	285	115

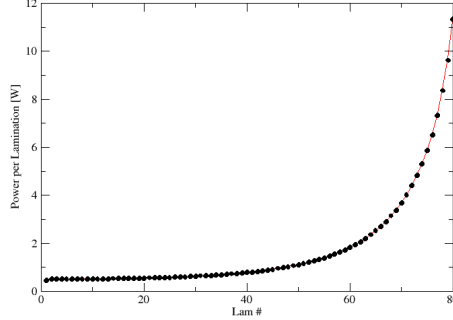


Figure 12: The average power dissipation in each of the 80 laminations of the quadrupole, when the quadrupole runs in an AC mode steady state at a frequency of 135 Hz. The power dissipation in each of the other 80 laminations is a mirror image of this plot.

320 duty cycle of quadrupole under normal operation is $\sim 1/40^{th}$ of that during
 321 the AC steady state operation of the quadrupole at $f=135$ Hz and $I_{max}=185$
 322 A. The power dissipation is small enough and the heat can be abducted by
 323 the method mentioned earlier in this paper.

324 *5.2. The effect of the eddy currents in the vacuum pipe on the field of the*
 325 *circulating beam region*

326 The vacuum pipe of the circulating beam has been included in the
 327 OPERA model and the effect of the eddy currents generated in the vac-
 328 uum pipe on the B-field of the circulating beam region was calculated.
 329 This effect on the B-field and some of the results from these calculations are
 330 presented in this section.

331 Fig. 13 shows $1/8^{th}$ of the magnets's model with the vacuum pipe which has
 332 been segmented into four sections, each 4 cm long, along the length of the
 333 quadrupole as shown in Fig. 13 to allow the calculation of the power loss due
 334 to the eddy currents in each 4 cm long section of the pipe instead of the
 335 whole 2X16 cm length of the pipe.

336 Table 4 tabulates some of the geometrical and physical properties of the
 337 vacuum chamber and the power loss in vacuum pipe due to the eddy currents.
 338 To obtain a better information on the power loss in the vacuum pipe, the
 339 pipe was segmented in 4 cm length of 8 segments in total (four sections up-
 340 stream and four sections downstream). The power loss in the four upstream

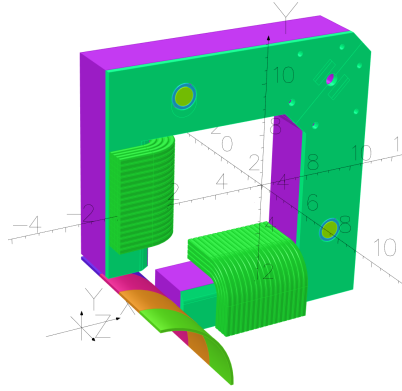


Figure 13: Some geometrical and physical properties (first three columns) of the vacuum pipe. The average power dissipation in each of the four 4 cm in length rings of the vacuum pipe appears in the last four columns.

Table 4: Geometric and material properties of Vacuum pipe

R_{inner} [cm]	$Wall_{thick}$ [cm]	σ [Siem/m]	Average Power dissipation per section			
			Sec1 [W]	Sec2 [W]	Sec3 [W]	Sec4 [W]
7.46	0.26	7.4×10^6	596	448	148	32

341 segments, starting from the segment at the center of the magnet appears in
 342 the last four columns of Table 4. This power dissipation corresponds to a
 343 steady state operation of the quadrupole at a frequency $f=135$ Hz.

344 It is noticeable as expected that the power dissipation in the vacuum pipe is
 345 reduced with the distance from the center of the magnet. The heat generated
 346 from this Ohmic power loss will partly be abducted by the cooler part of the
 347 pipe upstream and downstream of the magnet. Regarding the effect of the
 348 eddy currents on the B-field of the main field region Fig. 14 plots the B-field
 349 at a radius $R=1$ cm, starting from the center of the magnet up to a distance
 350 30 cm from the center. The integrated field difference between the two plots,
 351 one with conducting pipe made of inconel material the other without pipe,
 352 is 7.4%. Thus the eddy currents generated in the 2.6 mm thick vacuum pipe
 353 reduces the integrated quadrupole strength by 7.4% and changes the phase
 354 between Voltage and Current by 20° .

355 Although it appears that the Ohmic losses on the vacuum pipe due to the
 356 eddy-currents are very large close to 2.45 kW as calculated based on the
 357 steady state operation of the magnet at a frequency of 135 Hz the actual

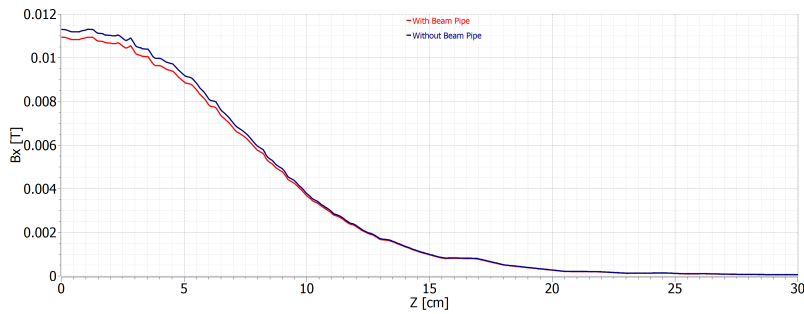


Figure 14: Plots of the B-field at R=1 cm from the reference orbit of the quadrupole for two cases. One without a vacuum pipe and the other with a 2.6 mm vacuum pipe made of inconel.

358 power dissipation is less than 100 W. In addition this power can be abducted
 359 by the cooler part of the vacuum chamber upstream and downstream of the
 360 quadrupole.

361 To complete the discussion of this section we refer the reader to Fig. 15 which
 362 shows the contour plots of the eddy currents on part of the vacuum pipe on
 363 the left picture. The right picture shows the direction of the current density
 of the eddy currents on the area enclosed by the little circle. -

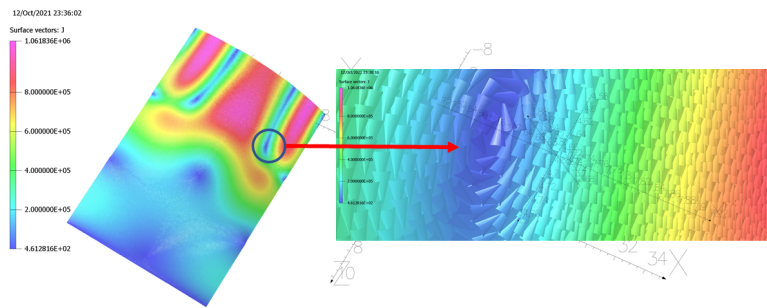


Figure 15: Counter plot of the density of the Eddy current in the pipe at particular time during the AC cycle. Only one eighth of the pipe is shown. The part of the pipe which is inside the quadrupole shows the highest current density. The right picture is a magnification of the part of the pipe enclosed by the circle and shows with arrows the direction of the currents.

364

365 **6. Conclusions**

366 A skew quadrupole has been designed to operate in a transient mode
367 during the AGS cycle. The magnetic core of the quadrupole was made of
368 iron laminations of 0.025” thick which are held by two iron plates 0.25”
369 thick.

370 The Ohmic losses during the actual operation of the quadrupole are low
371 enough for the coil to be air cooled with only a copper mass in contact with
372 the coil as a preventive mean for the coil to absorb any heat which might
373 harm the operation of the quadrupole. The strength of the 12-pole multipole
374 which is the first allowed multipole of the quadrupole is calculated to be
375 negligible.

376 The eddy currents generated in the 3.6 mm thick inconel vacuum pipe cause
377 a 7.4% reduction of the integrated quadrupole field. The Ohmic losses in
378 the vacuum pipe generate less than 100 W of heat during the operation of
379 the quadrupole. This heat can be absorbed by the rest of the pipe which has
380 lower temperature.

381 **7. References**

- 382 [1] <https://journals.aps.org/prl/pdf/10.1103/PhysRevLett.99.154801>
383 DOI: 10.1103/PhysRevLett.99.154801
- 384 [2] DOI: 10.1103/PhysRevSTAB.17.081001
385 <https://accelconf.web.cern.ch/IPAC2012/papers/TUXA03.PDF>
- 386 [3] “Using betatron coupling to suppress horizontal intrinsic spin resonances
387 driven by partial snakes”
388 V. Schoefer
389 DOI: 10.1103/PhysRevAccelBeams.24.031001
390 Brookhaven National Laboratory, Upton, New York
- 391 [4] <https://www.3ds.com/products-services/simulia/products/opera/>
392
- 393 [5] <https://www.bnl.gov/eic/>
394
- 395 [6] <https://journals.aps.org/prab/pdf/10.1103/PhysRevSTAB.16.043501>
396 DOI: 10.1103/PhysRevSTAB.16.043501

397
398

<https://accelconf.web.cern.ch/IPAC2012/papers/tuppc063.pdf>